Optics Letters

Experimental realization of dark and antidark diffraction-free beams

Xinlei Zhu,[1] Fei Wang,[1,5] Chengliang Zhao,[1] Yangjian Cai,[1,2,6] and Sergey A. Ponomarenko[3,4]

[1]School of Physical Science and Technology & Collaborative Innovation Center of Suzhou Nano Science and Technology, Soochow University, Suzhou 215006, China
[2]Shandong Provincial Engineering and Technical Center of Light Manipulations & Shandong Provincial Key Laboratory of Optics and Photonic Device, School of Physics and Electronics, Shandong Normal University, Jinan 250014, China
[3]Department of Electrical and Computer Engineering, Dalhousie University, Halifax, Nova Scotia B3J 2X4, Canada
[4]Department of Physics and Atmospheric Science, Dalhousie University, Halifax, Nova Scotia B3H 4R2, Canada
[5]e-mail: wangfei.phy@163.com
[6]e-mail: yangjiancai@suda.edu.cn

Received 13 March 2019; accepted 29 March 2019; posted 3 April 2019 (Doc. ID 362288); published 24 April 2019

We report the first, to the best of our knowledge, experimental realization of high-quality dark and antidark diffraction-free beams, first theoretically proposed by Ponomarenko *et al.* [Opt. Lett. 32, 2508 (2007)]. Our method employs a single spatial light modulator (SLM) and is based on superposing mutually uncorrelated but spatially coherent in the time domain Bessel modes with modal weights proportional to the SLM display times of the corresponding modes. We also experimentally verify diffraction-free properties of the generated beams upon their free space propagation.

https://doi.org/10.1364/OL.44.002260

To date, the most extensively studied partially coherent sources are of the so-called Schell-model type which give rise to uniformly correlated partially coherent beams [1]. The Schell-model sources can be readily realized in the laboratory using random phase spatial light modulators [2], or taking advantage of coherence shaping of free space propagating beams generated by incoherent light sources [1].

Although theoretical exploration of non-uniformly correlated partially coherent sources was initiated more than a decade ago [3], only a few examples of such sources have been studied in detail to date [3–6]. This is because laboratory realization of non-uniformly correlated partially coherent beams has met formidable difficulties. In fact, only one class of non-uniformly correlated partially coherent beams, composed of just two uncorrelated coherent modes, was experimentally realized very recently [7].

However, recent years have witnessed tremendous progress toward the experimental synthesis of partially coherent sources [8–15]. In particular, several approaches have been advanced to engineer non-uniformly correlated sources via linear superpositions of uncorrelated coherent modes. Specifically, the original non-uniformly correlated partially coherent source with a separable phase [3] was synthesized through a linear superposition of uncorrelated Laguerre–Gaussian modes by the Korotkova group [16]. Further, Ostrovsky *et al.* reported the experimental realization of a class of non-uniformly correlated diffraction-free partially coherent sources employing a specially designed Fourier transforming optical system with a spatial light modulator (SLM) [6]. The non-uniformly correlated sources of [6] are composed of diffraction-free Bessel modes with different wavenumbers and the same mode index. Interestingly, partially coherent dark and antidark diffraction-free sources, introduced by Ponomarenko and co-workers some time ago [4], are comprised of Bessel modes with an identical wavenumber but different mode indices. To the best of our knowledge, dark and antidark diffraction free beams have never been experimentally realized. We stress that the method of [6] is inapplicable to generating such sources because the angular spectra of the constitutive Bessel modes are not separable in a Fourier space.

In this Letter, we report the first, to the best of our knowledge, generation of dark and antidark diffraction-free sources using the coherent-mode superposition of Bessel modes. Each individual mode is generated by a laser beam, transmitted through a computer-generated hologram (CGH) loaded to an SLM. Dark or antidark diffraction-free beams are then obtained by averaging over temporal sequences of their coherent modes. We note that the weight of an individual mode in the superposition is proportional to the display time of the mode and is not interpreted as the probability of the mode appearance, thereby distinguishing our approach from that of previous work [6].

Let us first briefly review the salient features of dark/antidark diffraction-free sources [4]. The authors of [4] showed that the cross-spectral density of dark and antidark diffraction free beams, generated by such sources, takes the form

$$W(\boldsymbol{\rho}_1,\boldsymbol{\rho}_2) = J_0(\beta|\boldsymbol{\rho}_1 - \boldsymbol{\rho}_2|) + \alpha J_0(\beta|\boldsymbol{\rho}_1 + \boldsymbol{\rho}_2|), \quad (1)$$

where $\boldsymbol{\rho}_1$ and $\boldsymbol{\rho}_2$ are two arbitrary position vectors in the transverse plane of the beam; α and β are two real constants, and J_0 is a Bessel function of the first kind and order zero. Notice that the cross-spectral density is independent of the propagation distance z from the source, highlighting the diffraction-free nature of the beams. The analysis reveals that whenever $\alpha < 0$,

the spectral density of the beam has a dark notch on the axis against a bright background halo, whereas the case $\alpha > 0$ corresponds to the beam spectral density attaining a maximum (antidark bump) on top of a bright background.

Further, applying the following summation theorem for the Bessel functions,

$$J_0(\beta|\boldsymbol{\rho}_1 \mp \boldsymbol{\rho}_2|) = \sum_{m=-\infty}^{\infty} (\pm 1)^m e^{im(\phi_2-\phi_1)} J_m(\beta\rho_1) J_m(\beta\rho_2), \quad (2)$$

with (ρ_i, ϕ_i) $(i = 1, 2)$ standing for the polar coordinates, we obtain for the cross-spectral density of our dark/antidark beams the following coherent mode representation:

$$W(\boldsymbol{\rho}_1, \boldsymbol{\rho}_2) = \sum_{m=-N}^{m=N} \lambda_m \psi_m^*(\boldsymbol{\rho}_1, z) \psi_m(\boldsymbol{\rho}_2, z), \quad (3)$$

Here N denotes the number of modes that approaches infinity in theory; $\psi_m(\boldsymbol{\rho}, z) = J_m(\beta\rho) e^{im\phi} e^{iz\sqrt{k^2-\beta^2}}$ are the Bessel modes of the order m, and the mode weights are given by the expression [4]

$$\lambda_m = 1 + (-1)^m \alpha. \quad (4)$$

We infer at once that Eq. (3) constitutes a coherent mode representation of any physically realizable dark/antidark diffraction free beam, provided the magnitude of α is less than unity to guarantee non-negative definiteness of the cross-spectral density. Note also that each mode is an exact solution to the Helmholtz equation and z-dependent phase factors $e^{iz\sqrt{k^2-\beta^2}}$ have no effect on the beam cross-spectral density as they cancel out for each product of a coherent mode function and its complex conjugate entering the superposition of Eq. (3).

Let us now turn our attention to the experimental realization of the just described dark and antidark diffraction-free beams. In Fig. 1, we sketch our experimental setup. A linearly polarized He–Ne laser beam ($\lambda = 632.8$ nm), transmitted through a neutral density filter (NDF) and a beam expander (BE), was reflected by a mirror (RM) prior to arriving at a transmission only SLM (Holoeye 2008) with 1024×768 pixels (pixel sizes 36 μm × 36 μm). The SLM acted as a phase screen (hologram) used to generate coherent Bessel modes. The generated Bessel beam quality directly affected the quality of partially coherent beams. As ideal Bessel beams carrying infinite energy, which cannot be experimentally realized, their truncated counterparts were employed. To this end, we softly apertured ideal Bessel beams with a Gaussian filter function, yielding approximately non-diffracting Bessel–Gauss beams.

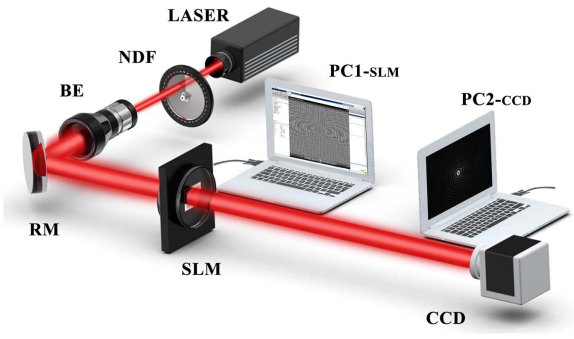

Fig. 1. Experimental setup for generating dark and antidark diffraction-free beams. NDF, neutral density filter; BE, beam expander; RM, reflecting mirror; SLM, spatial light modulator; PC, personal computer.

To produce high-quality Bessel beams with this holographic technique, we followed the procedure of [17]. We computed a phase pattern for converting a plane wave into a Bessel beam of the order m according to the prescription, $\varphi(\boldsymbol{\rho}) = m\varphi + \pi H[J_m(\beta\rho)]$, where H stands for a unit step-function. We then imparted a phase shift of $k_0 x$ to the computed phase with a blazed phase grating with the grating frequency k_0. As the resulting phase pattern was loaded to the SLM, the phase value fell into the interval between 0 and 2π. In Figs. 2(a) and 2(b), we illustrate typical phase patterns for thus generated Bessel modes with the mode indices $m = 4$ and 10, respectively. The first diffraction order of SLM was regarded as our Bessel mode. To ensure only the first-order diffracted beam reaches a CCD, we placed a circular aperture—not shown in the schematics of Fig. 1—to block the unwanted light. The CCD was placed right after the aperture to record the beam patterns.

In Figs. 2(c) and 2(d), we present the normalized intensity distributions of Bessel beams with $m = 4$ and 10 captured by the CCD. We also display the intensity distribution at the cross line ($y = 0$) in and the corresponding theoretical fit with ideal Bessel modes in Figs. 2(e) and 2(f) for comparison. We observe that the experimental results are virtually indistinguishable from the theoretical ones, at least up to the fourteenth concentric ring away from the beam center. Outside the fourteenth concentric ring, though, the measured mode intensity decays much faster than that predicted by the theory. This discrepancy is caused by our using Gaussian apertured Bessel modes in the experiment as opposed to the ideal Bessel modes. We can also infer the transverse wavenumber β magnitude from a theoretical fit is about 0.00245 k. This parameter can be changed through re-designing the phase grating.

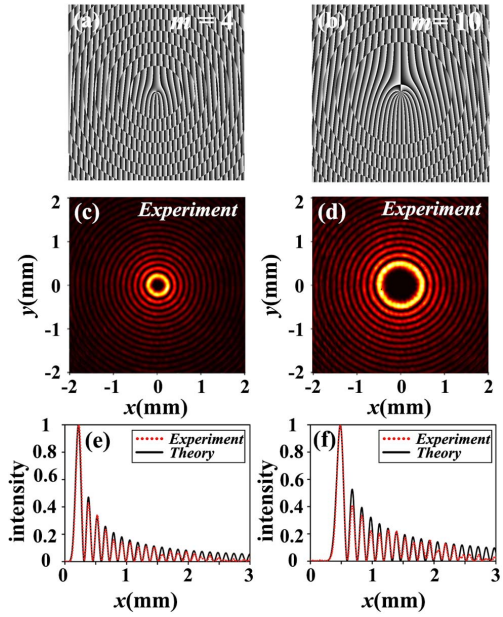

Fig. 2. (a) and (b) Phase patterns loaded to the SLM for generating softly apertured Bessel beams with $m = 4$ and $m = 10$; (c) and (d) Experimental results for the generated Bessel beams captured by the CCD; (e) and (f) cross lines for the generated beams at $y = 0$ and the corresponding theoretical fit.

After generating a series of Bessel modes of different orders m, we can now synthesize dark or antidark diffraction-free beams through incoherent superpositions according to Eq. (3). Previous numerical estimates indicate that a superposition of the first 51 modes ($N = 25$) gives a reasonably good approximation to a theoretical dark/antidark beam in the vicinity of the first beam notch/peak [4]. In the experiment, we chose $N = 31$, i.e., 63 Bessel modes of different orders were employed. Accordingly, we synthesized 63 phase patterns in the computer and loaded them to the SLM by rolling animation. In Fig. 3, we sketch the phase pattern loading sequence. At each time step, the chronologically earliest screen was removed from the computer memory and replaced by a new screen. The display time of each pattern was proportional to the desired mode weight factor λ_m. Thus, in our approach, we can readily control the mode weights through adjusting the display time of each phase pattern. The average frame per second (fps) rate of the phase pattern sequence loaded to the SLM was about 30 s^{-1}, which is lower than the maximum SLM refreshing rate of 60 Hz. We then obtained the dark/antidark diffraction-free beam intensity by averaging over the picture sequences of the Bessel modes captured by the CCD. The number of pictures used in the experiment was about 1200, and the averaging was performed offline.

In Figs. 4(a)–4(d), we present the density plots of the generated antidark ($\alpha = 1.0$, 0.5) and dark ($\alpha = -0.5$, -1.0) diffraction-free beam intensity distributions in the source plane. In Figs. 4(e) and 4(f), we also exhibit the experimentally obtained intensity distributions at the cross line ($y = 0$) and the corresponding theoretical results calculated from Eq. (3) by taking $\rho_1 = \rho_2$ with $N = 31$. As is evidenced by Fig. 4, for the positive values of α, 1.0 or 0.5, the intensity pattern displays a bright spot at the center, surrounded by several relatively dark concentric rings, while the intensity between the adjacent rings does not fall all the way to zero. Rather, the beam appears to reside on a uniform plane wave background, which is a signature of an antidark beam. As the value of α decreases, the solid bright core gradually disappears, and the uniform background brightness is enhanced. Eventually, as the limiting value $\alpha = -1$ is attained, the intensity at the beam center reaches zero as the antidark beam turns into a dark one.

We infer from Figs. 4(e) and 4(f) that our experimental results agree quite well with the theoretical ones. Outside the tenth ring, though, the intensity decays much faster than predicted by the theory and the concentric rings gradually disappear. This is the consequence of our using a finite number of Bessel modes in the experiment to approximate the ideal theoretical dark/antidark diffraction-free beams composed of an infinite number of modes. The agreement between the theory and experiment is excellent, however, in the most interesting region near the beam axis.

To verify the non-diffractive nature of the generated beams, we plot the experimental results for the normalized beam intensity distributions with $\alpha = 1$ and $\alpha = -1$ at three propagation distances, as seen in Figs. 5 and 6. As is expected, the beam shape and size remain nearly invariant after the propagation

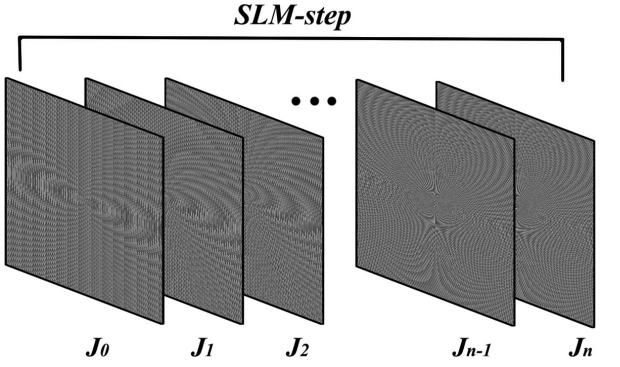

Fig. 3. Schematic illustration of the phase pattern sequence for Bessel mode generation with the SLM.

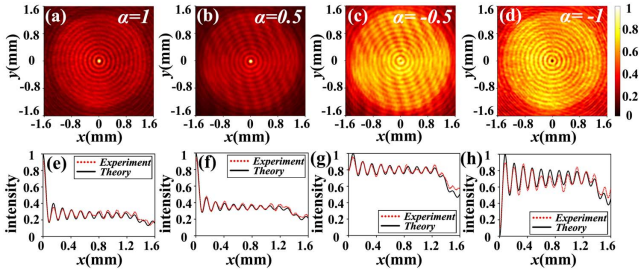

Fig. 4. (a)–(d) Experimental results for the normalized antidark/dark beam intensity patterns with $\alpha = 1.0$, 0.5, -0.5, -1.0 in the source plane; (e) and (f) the intensity distribution along the line $y = 0$ (red dashed–dotted) and the theoretical fit (solid).

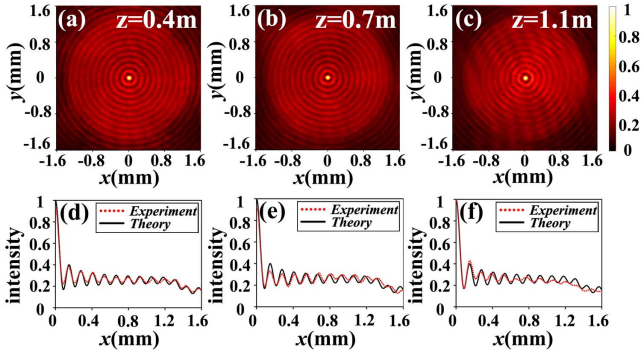

Fig. 5. (a)–(c) Experimental results for the normalized beam intensity distributions with $\alpha = 1$ at several propagation distances from the source plane; (d)–(f) the cross line ($y = 0$) experimental intensity distribution (red dashed–dotted) and the theoretical fit (solid).

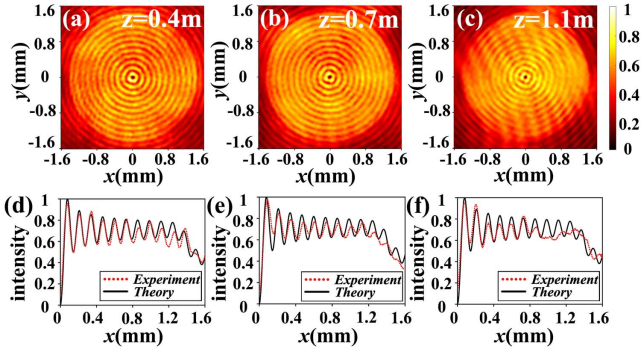

Fig. 6. (a)–(c) Experimental results for the normalized beam intensity distributions with $\alpha = -1$ at several propagation distances from the source plane; (d)–(f) the cross line ($y = 0$) experimental intensity distribution (red dashed–dotted) and the theoretical fit (solid).

distance of $z = 1.1$ m, with only a slight deviation from the theory detectable toward the beam tail after the sixth consecutive ring. If we are only interested in the region around the first bright spot of the antidark beam with $\alpha = 1$—the spot width is about 0.08 mm—or the first notch vicinity of the dark beam with $\alpha = -1$, the corresponding regions of the realized beams at distance $z = 1.1$ m are identical in shape and size to their counterparts in the source plane. We point out, for comparison, that a fundamental Gaussian beam of the initial width $w_0 = 0.08$ mm at the same carrier wavelength will spread to about three times its size in the source plane over the same propagation distance.

In conclusion, we have experimentally realized dark and antidark diffraction-free beams by designing uncorrelated superpositions of Bessel modes with the aid of an SLM, and we verified diffraction-free nature of the generated beams. We controlled the weight of each mode in the coherent mode representation of the beam cross-spectral density by adjusting the SLM display time of specially engineered phase holograms. Our method allows for a convenient transition from antidark to dark diffraction-free beams. We note that our modal weight control method is different from that reported in Ref. [16]. We also note that the present non-uniformly correlated beams are very different from the recently introduced, and experimentally realized, radially/circularly uniformly correlated partially coherent beams composed of Bessel modes [18–20]. The dark and antidark diffraction-free beams may find applications to optical trapping and manipulation of atoms or micro-particles.

Funding. National Natural Science Foundation of China (NSFC) (11525418, 11774250, 11874046, 91750201); Priority Academic Program Development of Jiangsu Higher Education Institutions; Qing Lan Project of Jiangsu Province.

REFERENCES

1. L. Mandel and E. Wolf, *Optical Coherence and Quantum Optics* (Cambridge University, 1995).
2. N. R. Zandt, M. W. Hyde, S. R. Bose-Pillai, D. G. Voelz, X. Xiao, and S. T. Fiorino, Opt. Commun. **387**, 377 (2017).
3. S. A. Ponomarenko, J. Opt. Soc. Am. A **18**, 150 (2001).
4. S. A. Ponomarenko, W. Huang, and M. Cada, Opt. Lett. **32**, 2508 (2007).
5. H. Lajunen and T. Saastamoinen, Opt. Lett. **36**, 4104 (2011).
6. A. S. Ostrovsky, J. Garcia-Garcia, C. Rickenstorff-Parrao, and M. A. Olvera-Santamaria, Opt. Lett. **42**, 5182 (2017).
7. G. V. Bogatyryova, C. V. Felde, P. V. Polyanskii, S. A. Ponomarenko, M. S. Soskin, and E. Wolf, Opt. Lett., **28**, 878 (2003).
8. P. D. Santis, F. Gori, G. Guattari, and C. Palma, J. Opt. Soc. Am. A **3**, 1258 (1986).
9. M. W. Hyde IV, S. R. Bose-Pillai, and R. A. Wood, Appl. Phys. Lett. **111**, 101106 (2017).
10. M. W. Hyde IV, S. Basu, D. G. Voelz, and X. F. Xiao, J. Appl. Phys. **118**, 093102 (2015).
11. Y. Chen, S. A. Ponomarenko, and Y. Cai, Appl. Phys. Lett. **109**, 061107 (2016).
12. F. Wang, X. Liu, Y. Yuan, and Y. Cai, Opt. Lett. **38**, 1814 (2013).
13. Y. Chen, S. A. Ponomarenko, and Y. Cai, Sci. Rep. **7**, 39957 (2017).
14. C. Liang, G. Wu, F. Wang, W. Li, Y. Cai, and S. A. Ponomarenko, Opt. Express **25**, 28352 (2017).
15. S. Avramov-Zamurovic, C. Nelson, S. Guth, and O. Korotkova, Appl. Opt. **55**, 3442 (2016).
16. X. Chen, J. Li, S. M. H. Rafsanjani, and O. Korotkova, Opt. Lett. **43**, 3590 (2018).
17. N. Matsumoto, T. Ando, T. Inoue, Y. Ohtake, N. Fukuchi, and T. Hara, J. Opt. Soc. Am. A **25**, 1642 (2008).
18. M. Santarsiero, R. Martinez-Herrero, D. Maluenda, J. C. G. Sande, G. Piquero, and F. Gori, Opt. Lett. **42**, 1512 (2017).
19. G. Piquero, M. Santarsiero, R. Martinez-Herrero, J. C. G. Sande, M. Alonzo, and F. Gori, Opt. Lett. **43**, 2376 (2018).
20. M. Santarsiero, R. Martinez-Herrero, D. Maluenda, J. C. G. Sande, G. Piquero, and F. Gori, Opt. Lett. **42**, 4115 (2017).